Radiol Phys Technol (2011) 4:164–172
DOI 10.1007/s12194-011-0117-2

Development of quality control system for flat-panel detectors

Atsushi Teramoto · Takahiko Kajihara · Shoichi Suzuki · Kazuo Kinoshita · Masatoshi Tsuzaka · Hiroshi Fujita

Received: 7 September 2010 / Revised: 2 March 2011 / Accepted: 3 March 2011 / Published online: 17 March 2011
© Japanese Society of Radiological Technology and Japan Society of Medical Physics 2011

Abstract The characteristics of flat-panel detectors (FPD) are degraded by exposure to radiation. Degradation in a FPD progresses locally and has a nonlinear relationship to the radiation dose. In order to manage FPD systems properly, one must perform quality control (QC) such as evaluation of image degradation. However, no evaluation method for degradation has been established. In this paper, we first review the structure and degradation mechanism of FPDs, and then we propose a daily QC system for FPDs. To evaluate the degradation of FPDs, we investigated the number of defective pixels and lines, as well as the offset level of the pixel output. Furthermore, we developed daily QC software for FPD that can evaluate the image quality and is operationally simple. In the experiments, an indirect-conversion type FPD was evaluated by our proposed system. The offset level of FPD increased exponentially with X-ray exposure; no trends were seen for the number of defective pixels and defective lines. The required time for the evaluation of an FPD was about 1 min, and no special skills were needed for the analysis. These results indicate that our system may be useful for daily QC of FPDs.

Keywords Flat-panel detector (FPD) · Quality control · Computer analysis · Imaging property

1 Introduction

Flat-panel detectors (FPDs) [1, 2] are widely used as imaging devices in X-ray diagnostic systems. They contain wide-area semiconductor components which form the final image. FPDs have the advantages of having good anti-distortion, dynamic range, and efficiency characteristics. However, as with other imaging devices, their image characteristics are degraded with use.

The semiconductors utilized in FPDs change their electrical characteristics due to the effects of radiation, and consequently, the input–output characteristics of the image also change [3–6]. Degradation of FPDs according to the radiation dose is seeing accelerating progress [4, 5]. Therefore, it is very difficult to decide on the component exchange times on the basis of the periodic checks recommended by the manufacturer.

Although exchange of FPDs is necessary following degradation, it is not easy to manage the sudden replacement costs because the units are very expensive. Therefore, in order to manage an FPD system properly by understanding the degree of their degradation, we think it is very important for radiological technologists to perform daily quality control (QC) of the FPD system.

A part of this study was reported at the 65th and 66th general meeting of the JSRT.

A. Teramoto (✉) · T. Kajihara · S. Suzuki
Faculty of Radiological Technology, School of Health Sciences, Fujita Health University, 1-98 Dengakugakubo, Kutsukake-cho, Toyoake, Aichi 470-1192, Japan
e-mail: teramoto@fujita-hu.ac.jp

K. Kinoshita
Department of Radiology, Banbuntane Soutokukai Hospital, 3-6-10 Ogashirabashi, Nakagawa-ku, Nagoya, Aichi 454-8509, Japan

M. Tsuzaka
Department of Radiological Technology, School of Health Sciences, Nagoya University, 1-1-20 Daikominami, Higashi-ku, Nagoya, Aichi 461-8673, Japan

H. Fujita
Department of Intelligent Image Information, Graduate School of Medicine, Gifu University, 1-1 Yanagido, Gifu, Gifu 501-1194, Japan

QC for medical imaging devices involves evaluation of image properties for certain minimum levels of image quality. The evaluation method is determined based on the structure and characteristics of a device. As for the evaluation of image properties, numerous results have been reported [7–10]. The initial performance of medical FPD systems was evaluated with use of existing evaluation methods [modulation transfer function (MTF), noise power spectrum (NPS), and signal-to-noise ratio]. However, existing evaluation methods are not applicable to the evaluation of FPDs because the degradation of FPDs advances locally.

In this study, we focused on a QC method specially designed for FPDs, which deals with local and nonlinear progression of degradation. Our goal in this study was to evaluate the degradation of FPDs, and then to develop a daily QC system which would be able to estimate the required exchange time based on the trend of the degradation characteristics.

In this paper, we describe the first challenge, which is to review the structure and the degradation mechanism of FPDs, and then we propose methods for the detection of the degradation in FPDs. Subsequently, we use the proposed method to develop a system for day-to-day QC in the medical field. In the Sect. 3, the degradation characteristics of an indirect-conversion-type FPD were evaluated with use of software that we developed.

2 Materials and methods

2.1 Degradation of FPDs

The semiconductors utilized in FPDs change their electrical characteristics due to the effects of radiation, and consequently, the input–output characteristics of the image also change. Until now, there have been numerous studies on the radiation damage of image sensors [3–5]. For example, Boudry et al. [4] reported on the radiation damage to amorphous silicon photodiode sensors. They showed that the dark current of the photodiode rose rapidly after a certain radiation dose had been exceeded. Xiang-Ti et al. [5] reported similar results of an experiment in which they used gamma rays and electron beams. Regarding the degradation of FPDs, the dark current rose according to the radiation dose as well as the above-mentioned image sensors [6].

Basically, FPD equipment requires periodic calibration in which the system detects defects and incorporates their correction into a pre-processing algorithm, which corrects these defects, as well as compensates for the heel effect of the X-ray beam. However, the image properties (noise, resolution, and dynamic range) of the defective area are greatly degraded even though the image is corrected. Thus, it is very important to detect how degradation in FPDs progresses.

In this section, we first review the structure of indirect- and direct-conversion FPDs, and then we review the causes of degradation and the image characteristics resulting from the degradation. FPDs are classified as either indirect- or direct-conversion FPDs on the basis of their structure; the processes and locations of the degradation are different in the two types.

2.1.1 *Indirect-conversion FPDs*

An indirect-conversion FPD consists of a scintillator, a photodiode, a capacitor, and a charge-transport circuit. It is shown schematically in Fig. 1a. X-rays entering the device are converted to visible light in the scintillator, and this light is then converted to electrical charge in the photodiode. The charge is accumulated on the capacitor and is periodically transferred out by the charge-transport circuit. In indirect FPDs, degradation is mainly due to radiation effects; its occurrence in the various components is described in the following paragraphs.

2.1.1.1 Scintillator In the scintillator, because of coloring by the radiation, pixel values are decreased, which causes a loss of dynamic range and an increase in the noise level.

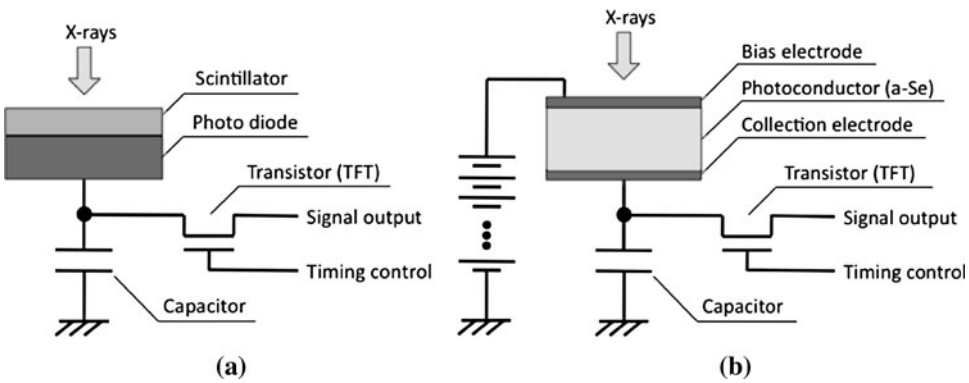

Fig. 1 Structure of **a** indirect-conversion FPD and **b** direct-conversion FPD

2.1.1.2 Photodiode [3–5] Degradation of the photodiode occurs near the oxide film as a result of the accumulation of electron holes which are produced by the ionizing radiation, and the dark current in the photodiode increases. These holes easily accumulate in the region of residual defects introduced during the semiconductor manufacturing process, and the increase in the dark current generally occurs locally. Due to the increase in the dark current, the region of the image where the pixel values increase becomes noticeable.

2.1.1.3 Charge-transport transistor [3–5] The transistor in the charge-transport circuit can also be damaged by ionizing radiation, and as a consequence, the pixel values fluctuate, or dot or line defects appear.

2.1.2 Direct-conversion FPDs

Direct-conversion FPDs consist of an X-ray conversion film and a capacitor, in addition to a charge-transport circuit in the electrode, as shown as Fig. 1b. X-rays entering the device produce free charges (electrons and electron holes) in the X-ray conversion film, across which a high voltage is applied between the electrodes. The charge accumulates in the capacitor and is periodically transferred by the charge-transport circuit. In direct-conversion FPDs, degradation is principally the result of electrical discharge and heat, and it occurs mainly in the following components.

2.1.2.1 Charge-transport transistor [3–5] Similar to the case for the indirect-conversion FPD, this transistor is affected by the ionizing radiation, and the pixel values fluctuate, and dot or line defects appear.

2.1.2.2 X-ray conversion film [11] Increasing temperature in the FPD leads to a change in the crystal structure of the X-ray conversion film, which causes a fluctuation in the pixel value, leading to an increase in the noise level and a decrease in image sharpness.

2.1.3 Partial and total degradation of FPD

The degradation described in Sects. 2.1.1 and 2.1.2 can be classified according to whether it affects the entire image or some local region only, as shown in Table 1. Total degradation of FPDs can be evaluated by existing methods such as the MTF. However, total degradation is very rare, and partial degradation is the dominant effect. Figure 2 shows examples of images in which such partial degradation has occurred in an indirect-conversion FPD. Horizontal and vertical defect lines are shown in Fig. 2a. Although the defect lines also exist in the production process, their positions are registered and corrected by use of the nearest pixels. Defect lines occurring after shipment may be seen in the image. Figure 2b is the image with no X-ray input. There are some white regions in the image.

Table 1 Partial and total degradation of FPDs

Type	Degradation
Partial degradation	Increase of defect pixels
	Increase of defect lines
	Regional increase of offset level
Total degradation	Increase of noise level
	Decrease of sharpness

2.2 Detection algorithm for degradation conditions

In this section, we present a detection algorithm for the defect pixels and lines, and a detection algorithm for the degradation conditions caused by the rise of the offset level.

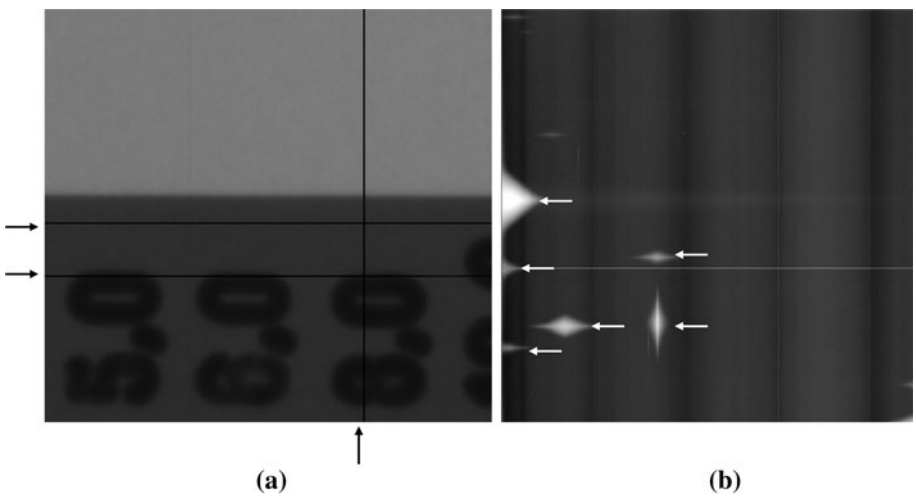

Fig. 2 Sample images of FPD degradation (indirect-conversion FPD). **a** Sample image with defect lines. *Arrows* show the defect lines. **b** Sample image with regional defects seen as *white regions* due to the increase in the dark current. *Arrows* show the regions of degradation

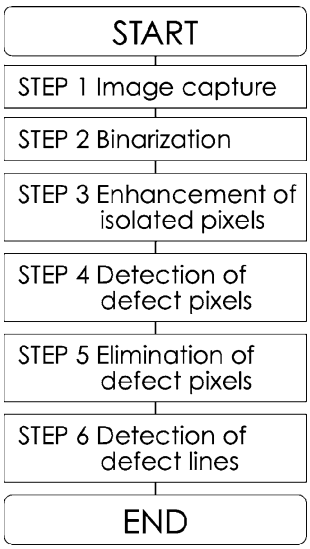

Fig. 3 Flow chart for detection of defect pixels and lines. After binarization of the captured image, isolated defect pixels are detected, and then defect lines are detected

2.2.1 Defect pixels and lines

A defect pixel is a dead pixel that contains no information. When a vertical or horizontal string of such pixels exists, it is referred to as a defect line. Here, in order to detect such structures, one calculates the number of defect pixels (NDP) and the number of defect lines (NDL). For the calculation of NDP and NDL, we introduce the following procedures.

In STEP 1 in Fig. 3, the image is captured under the condition in which there is no X-ray input into the FPD (Fig. 4a). Pixel values which do not have image information are observed at either drastically higher levels (high-level defect) or at lower levels (low-level defect) than the offset level.

Next, binarization is performed in STEP 2, and the defect pixel and the normal pixel are separated. Because the defect pixel has either a high or a low value, threshold values Th_1 for detection of high-level defects and Th_2 for detection of low-level defects are introduced. Regarding the threshold values, $Th_1 = D - Min/2$ and $Th_2 = Min/2$

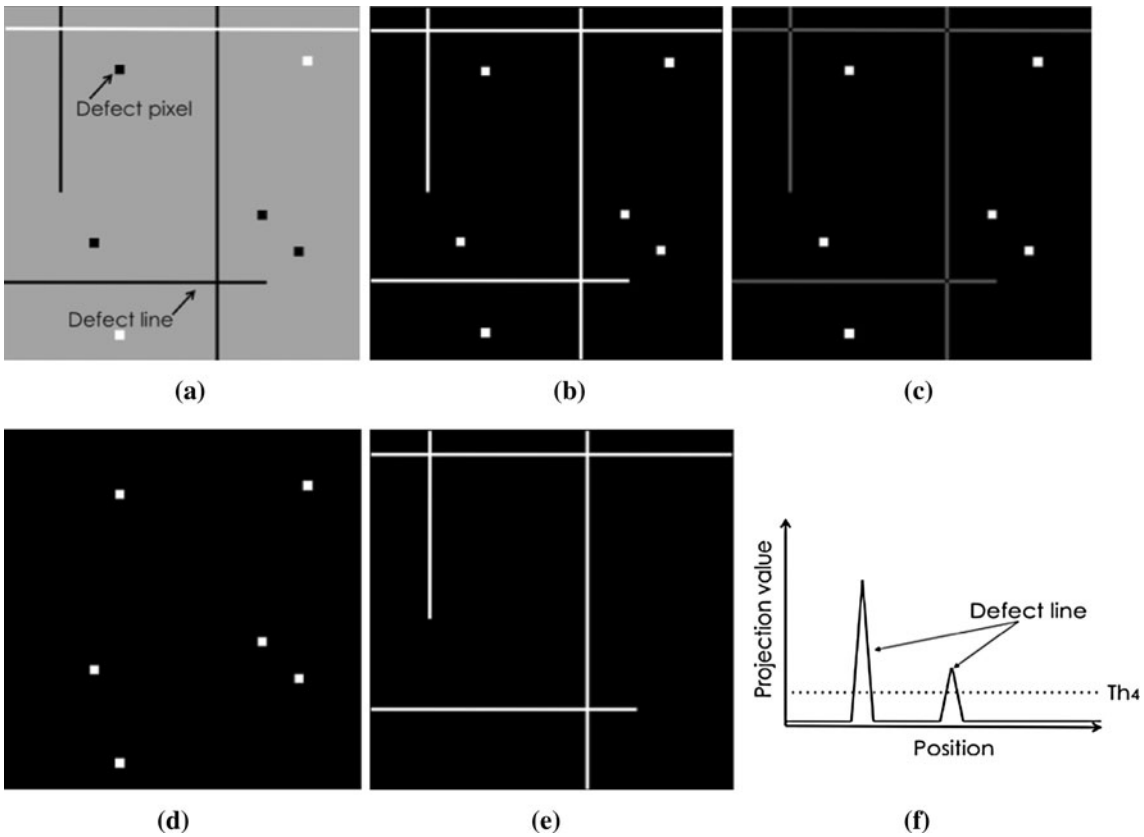

Fig. 4 Detection of defect pixels and lines. **a** Original image (STEP 1 in Fig. 3). **b** Binarization image (STEP 2). **c** Enhancement result of defect pixels (STEP 3). **d** Detection result showing defect pixels (STEP 4). **e** Elimination result of defect pixel from (**b**) (STEP 5). **f** Profile of the projection value and threshold, Th_4, for line-defect detection (STEP 6)

are applicable for indirect-conversion-type FPDs based on our experience (D, the number of the gray levels; Min, minimum offset level calculated by non-degraded pixel). When the pixel value is higher than Th_1 or lower than Th_2, the output pixel becomes 1; otherwise, the output is set to 0. As a result, the image containing defect pixels and defect lines is obtained, as shown in Fig. 4b.

In STEP 3, the extracted image is convolved by use of a Laplacian edge operator, and then the isolated defect pixels are enhanced (Fig. 4c).

In STEP 4, by performing another binarization using threshold Th_3 for the enhanced image, we can obtain an image which has only isolated pixels, as shown in Fig. 4d. An enhanced pixel shows the degree of isolation, which has a value between 0 and 8. If we evaluate the completely isolated pixels, $Th_3 = 8$ is adopted. $Th_3 = 1$–7 is adopted when we allow the connection of defect pixels. The positions of defect pixels are recorded, and the total number of defect pixels is defined as the NDP.

Next, STEP 5 deletes defect pixels from the defect-extracted image in Fig. 4c, so that the image contains only defect lines (Fig. 4e).

In STEP 6, by projection of the image vertically and horizontally, two sets of projection data are obtained. When there is the position that the projection value exceeds the threshold Th_4, this is considered a defect line, as shown in Fig. 4f. The total number of defect lines is defined as NDL. Here, Th_4 is equal to the length of the defect line which our method detects. The length of the defect line is sometimes shorter than half the length of the horizontal or vertical line. So, Th_4 is set at about 25–50% in the length of the horizontal or vertical line.

2.2.2 *Offset level*

As a result of long-term radiation exposure, the dark current in FPD pixels increases, and the pixel values rise locally as shown in Fig. 2b. This phenomenon is additive; the offset level rises locally, and the area of the degraded position also increases with the progress of the degradation.

Degradation with large area comparatively affects the diagnosis. In order to evaluate the degradation, we divided the image into multiple blocks, and by using the average pixel value for each block, we introduced a technique for evaluating the degree of increase over the initial value.

The procedure is explained below with reference to the flow chart of Fig. 5 and the image of Fig. 6. In STEP 1 in Fig. 5, obtain an image from the FPD in the absence of radiation, as shown in Fig. 6a. In this image, regions can be seen where the offset level has increased and defect pixels and lines are apparent.

Although the area occupied by defect pixels and lines is small in comparison to the region of increased offset level; this still leads to errors in the calculation of the offset level because of the high pixel values of the defect regions. For this reason, in STEP 2, the defect pixels and lines are removed from the image by use of the following procedure: first, erosion followed by dilation filtering is carried out on the original image (Fig. 6a) [12]. Defect pixels and lines that have high pixel values are eliminated by this process. Subsequently, dilation followed by erosion filtering is performed, which removes defect pixels and lines that have low pixel values. The resulting image shows only the variations in the offset level, as seen in Fig. 6b.

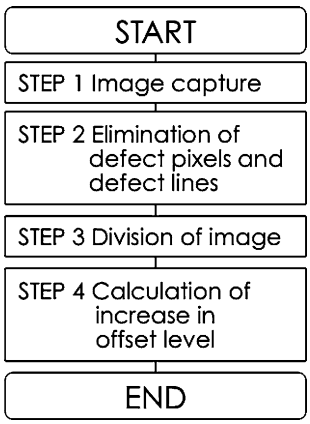

Fig. 5 Flow chart for detection of increase in offset level. First, defect pixels and defect lines are eliminated. After division the image into $M \times N$ small blocks, the increase in the offset level is calculated

In STEP 3, this image is then divided into $M \times N$ small blocks, and the average pixel value $P(M,N)$ in each block is calculated (Fig. 6c).

In STEP 4, the maximum value of the offset level (OL_{max}) and the mean value of the offset level (OL_{mean}) are calculated from the $P(M,N)$ data. Then, the increases IOL_{max} and IOL_{mean} in OL_{max} and OL_{mean} are calculated as follows:

$$IOL_{max} = \frac{OL_{max} - OL_{max}(0)}{D} \quad (1)$$

$$IOL_{mean} = \frac{OL_{mean} - OL_{mean}(0)}{D} \quad (2)$$

where $OL_{max}(0)$ and $OL_{mean}(0)$ are the OL_{max} and OL_{mean} when the image quality is accepted by an initial QC test, respectively. D is the number of gray levels of the FPD.

2.3 QC software for FPD system

For the purpose of easy QC of FPD in the medical field, we developed QC software by using a degradation detection algorithm (Fig. 7; Table 2). This system is a Windows-based application developed with use of Visual C++. The image formats supported are DICOM and RAW data (16 or 32 bits). Evaluation dates and results are stored in a comma-separated-value (CSV) file format, which allows

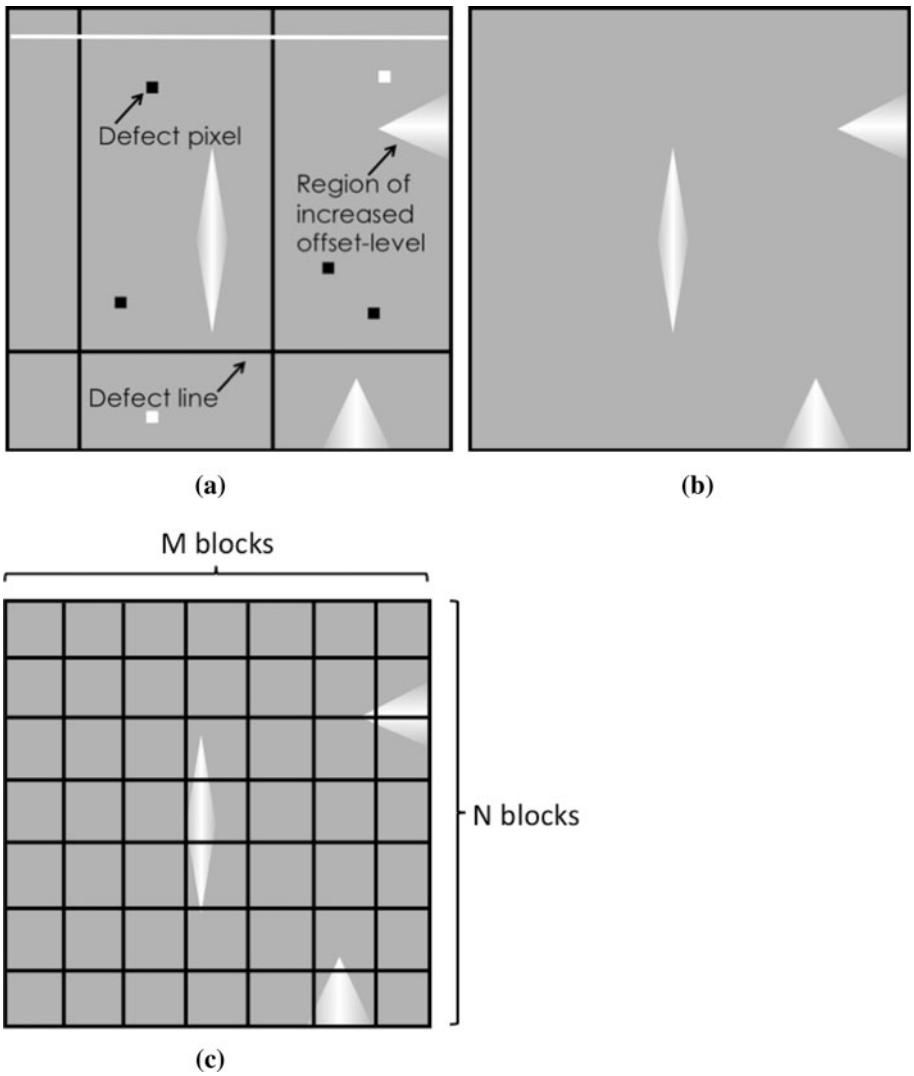

Fig. 6 Evaluation of degradation in FPD by use of increase in offset level. **a** Original image (STEP 1 in Fig. 5). **b** Image after the elimination of defect pixels and lines (STEP 2). **c** Division of the image into $M \times N$ small blocks (STEP 3)

the trend to be illustrated graphically with use of consumer software such as Excel.

3 Experiments and results

3.1 Evaluation method

We evaluated the degradation parameters with an actual FPD in order to confirm the effectiveness of this system. We evaluate OL_{max}, OL_{mean}, NDL, and NDP described in the last section, in order to identify the changes in characteristics caused by degradation. The specifications of the monitored FPD are shown in Table 3. We used an indirect-conversion FPD that was used for dental and industrial use; it has a CsI scintillator and a pixel pitch of 0.05 mm.

The FPD was irradiated with continuous X-rays at a tube voltage of 100 kV, a tube current of 0.03 mA, and with a source to image distance of 350 mm, resulting in a dose rate at the FPD surface of 2.29×10^{-5} (C/kg)/min. In the actual evaluation, irradiation was performed 8 h a day. Degradation parameters were measured after 8 h of irradiation. This evaluation was repeated for about 500 days. Then, the time-dependent variations in the degradation parameters were monitored.

In the calculation of $OL_{max,mean}$ and $IOL_{max,mean}$, The image segmentation number of the FPD shown in Fig. 6c was 20×20 (the matrix size of each block was 100×100 pixels). Threshold values Th_1–Th_4 for the calculation of NDP and NDL were set as follows: $Th_1 = 4070$, $Th_2 = 25$, $Th_3 = 8$, $Th_4 = 560$.

3.2 Results

Figure 8 shows the result. It was confirmed that OL_{max} increased exponentially with X-ray exposure. The value of OL_{max} was about 10 times larger than that of OL_{mean}, and the difference increased with the X-ray exposure. This

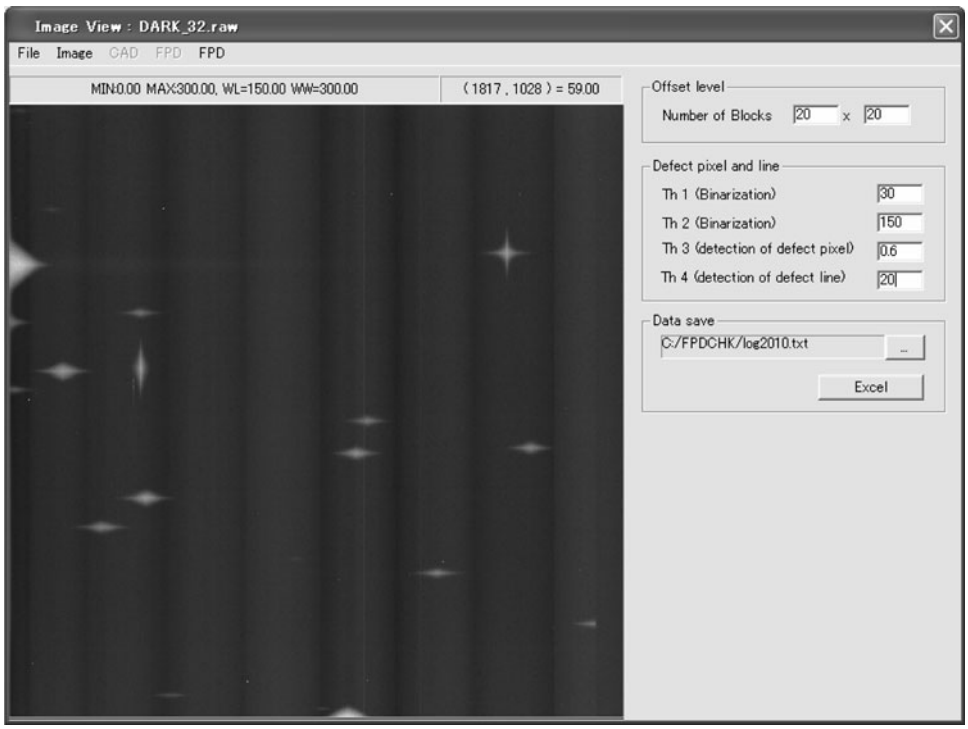

Fig. 7 FPD management software. Software was developed by use of Visual C++. All evaluations are easily performed by mouse operation

Table 2 Specification of FPD management software

Software	32-bit Windows application
Input image	DICOM, RAW (16 bits, 32 bits)
Evaluation items	NDP
	NDL
	OL_{max}
	OL_{mean}
Output data	CSV file (date, evaluation item, result)

Table 3 Specifications of the indirect-conversion FPD employed in our experiment

Panel name	C7942CA (Hamamatsu Photonics)
Scintillator	CsI
Number of pixels ($X \times Y$)	2240 × 2344
Pixel size (mm)	0.05
Digital output (bit)	12

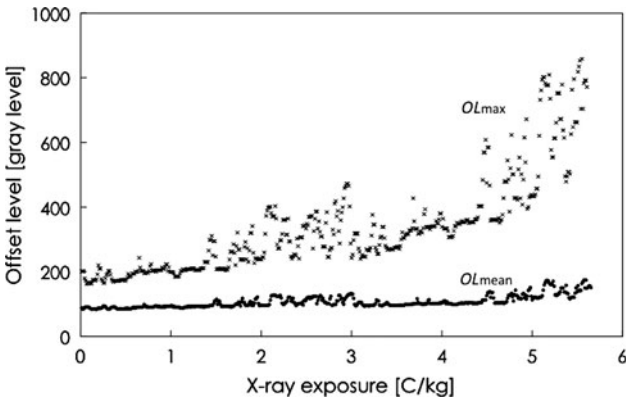

Fig. 8 Evaluation result showing the FPD offset level versus X-ray exposure. OL_{max} increases exponentially with X-ray exposure, but OL_{mean} remains almost constant

result indicates that the degradation of the FPD progresses locally. Figure 9 shows the characteristics of IOL_{max} and IOL_{mean}. Values at the endpoint of measurement were 13.9 and 1.49%, respectively.

Figure 10 shows the number of defect pixels and lines as a function of X-ray exposure. The number of defect lines is seen to be constant. Also, little or no trend is seen for the number of defect pixels. A considerable amount of scatter appears in this curve, which may be the result of changing environmental conditions such as ambient temperature, which cause fluctuations in the pixel values.

4 Discussion

In this paper, we propose a technique and system for daily QC based on detection of the degradation characteristics of FPDs. In the section on evaluating the degradation conditions, the offset level was observed to increase exponentially with X-ray exposure. The rise in the maximum offset level OL_{max} with irradiation was remarkable in comparison

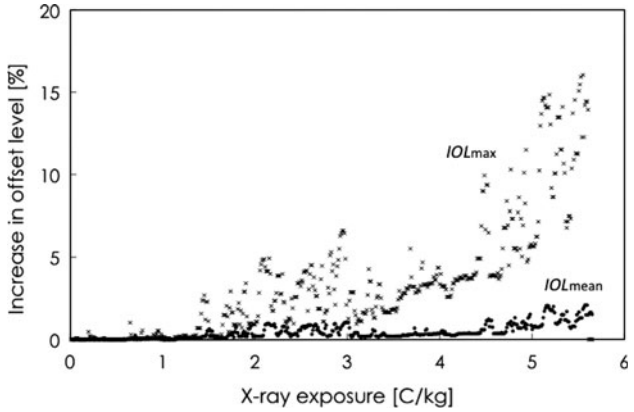

Fig. 9 Evaluation result of increase in offset level. IOL_{max} and IOL_{mean} at the endpoint of measurement were 13.9 and 1.49%, respectively

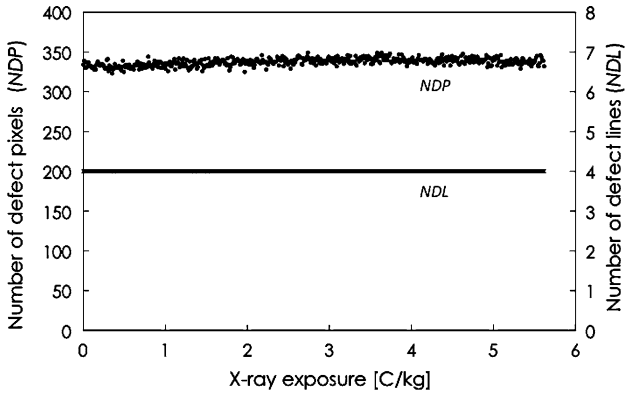

Fig. 10 Evaluation results of NDP and NDL. Both were almost constant regardless of X-ray exposure

with the average offset level OL_{mean}. Changes in the defect line and the defect pixel because of irradiation were not observed.

In indirect FPDs, the main process for the degradation is the rise in the offset level, and high doses seem to be necessary for increases in defect pixels and lines.

The numbers of the defect pixels displayed dispersion, that could have been caused by environmental conditions such as ambient temperature, which could be responsible for the fluctuations of the pixel values of the defect pixels. For the defect lines, stable results with no fluctuations were obtained.

It can be considered that, with the introduction of our pixel projection method for the detection of the defect lines, the effects of fluctuations on the pixel values are drastically minimized.

The evaluation time was only 1 min on the Intel Core2Quad Q8400 system with use of the special software that we developed. Furthermore, the only required operation was the reading of the image files. Thus, it seems that this procedure could conveniently be a part of a daily QC program.

5 Conclusion

In this paper, as an approach to managing the degradation in FPD systems, the degradation mechanisms were reviewed for both direct- and indirect-conversion FPDs, and a technique for quantifying the degree of degradation was proposed. In addition, QC software was developed that facilitates daily monitoring of the progress of FPD degradation.

We carried out an experiment to evaluate the trend of degradation in an indirect conversion FPD used for dental and industrial purposes. The results showed that the offset level increased exponentially with X-ray exposure. On the other hand, changes in the defect pixels and lines because of irradiation were not observed.

Finally, future challenges related to this technique are discussed. The main challenges are data storage and establishment of a self-diagnosis technique. In the future, the degradation status of FPD equipment will be measured continuously with this system. Based on these data, we will develop self-diagnosis software which will estimate the optimum exchange time by analyzing the trends in the degradation parameters.

A secondary challenge is the improvement of the data entry method. At present, the system uses RAW data with no image correction or frequency filtering. Because some systems cannot output the RAW data format, it is necessary to gain the cooperation of the manufacturer. In addition, the methods for acquiring degradation information from the images after correction must be re-examined for the situation where RAW data cannot be obtained.

References

1. Rowlands J, Kasap S Amorphous semiconductors usher in digital X-ray imaging. Phys Today. 1997:24–30
2. Moy JP. Large area X-ray detectors based on amorphous silicon technology. Thin Solid Films. 1999;337:213–21.
3. Hopkinson GR. Radiation effects on solid state imaging devices. Radiat Phys chem. 1994;43:79–91.
4. Boudry JM, Antonuk LE. Radiation damage of amorphous silicon photodiode sensors. IEEE Trans Nucl Sci. 1994;41:703–7.
5. Meng X-T, Kang A-G, Li J-H, Zhang H-Y, Yu S, Zheng Y. Effects of electron and gamma-ray irradiation on CMOS analog image sensors. Microelectron Reliab. 2003;43:1151–5.
6. Boudry JM, Antonuk LE. Radiation damage of amorphous silicon, thin-film, field-effect transistors. Med Phys. 1996;23: 743–54.
7. Siewerdsen JH, Antonuk LE, El-Mohri Y, Yorkston J, Huang W, CunninghamSiewerdsen IA. Signal, noise power spectrum, and

detective quantum efficiency of indirect-detection flat-panel imagers for diagnostic radiology. Med Phys. 1998;25:614–28.
8. Samei E, Flynn MJ. An experimental comparison of detector performance for direct and indirect digital radiography systems. Med Phys. 2003;30:608–22.
9. Samei E. Image quality in two phosphor-based flat panel digital radiographic detectors. Med Phys. 2003;30:1747–57.
10. Granfors PR, Aufrichtig R, Possin GE, Giambattista BW, Huang ZS, Liu J, et al. Performance of a 41×41 cm^2 amorphous silicon flat panel X-ray detector designed for angiographic and R&F imaging applications. Med Phys. 2003;30:2715–26.
11. Arthur SD, David SW. Handbook of imaging materials. New York: Marcel Dekker; 2001. p. 329–68.
12. Maragos PA, Schafer RW. Morphological filters-Part I: their set-theoretic analysis and relations to linear shift-invariant filters. IEEE Trans ASSP. 1987;35:1153–69.